© *Proc. Indian natn. Sci. Acad.*, **52**, A, No. 1, 1986, pp 265-291.
Printed in India.

DIVIDED METALS*

PETER P EDWARDS

University Chemical Laboratory, Lensfield Road, Cambridge CB2 1EW, U.K.

(*Received 6 December 1985*)

In this lecture, I intend to present a very brief overview of the question of the electronic structure of metals which are neither quite macroscopic, nor microscopic is nature. Our interest is these Divided Metals is motivated by the need to understand the metallic and nonmetallic states of matter, for it can be asserted that to understand either regime one must elucidate the manner in which bulk, macroscopic states of matter evolve from the progressive agglomeration of atomic constituents. Alternatively, Divided Metals can be viewed as arising from the bulk metallic phase *via* subdivision of a macroscopic solid.

The questions to raise, therefore, are both experimental and theoretical. How does one connect the microscopic world of atomic and molecular clusters with the macroscopic world of metals and insulators? In what manner can one probe experimentally the progressive evolution of bulk properties, as a function of number or size? and how does one begin to formulate a conceptual picture of this evolution? The present work, then, attempts to touch upon two such inter woven themes: metal-insulator transitions and the evolution of macroscopic states of matter from progressive agglomeration of their atomic siblings. The title of this talk originates from Faraday's work on gold in a metallic, divided state, published over a century ago.

INTRODUCTION

IN 1857, Michael Faraday presented his Bakerian Lecture entitled[1] "Experimental Relations of Gold (and Other Metals) to Light." Faraday's work on gold, silver and other metals led him to conclude that "... *the gold is reduced in exceedingly fine particles which becoming diffused, produce a beautiful fluid .... the various preparations of gold whether ruby, green, violet or blue....consist of that substance in a* **metallic divided state**"** A present day investigation[2] of metallic, divided gold—colloidal gold—can reveal just how close to the truth were Faraday's conceptions of the problem some 130 years ago. Fig. 1 (a) shows electron microscope photographs of submicron-sized colloidal gold particles prepared from the reduction of chlorauric acid with sodium citrate. In Fig. 1 (*b*) is shown a high resolution electron microscope picture of an individual gold particle in which one begins to see the detailed structure of the metal particle at the nanometer level.

*Presented at the INSA Golden Jubilee Symposium on Solid State Chemistry held at INSA during December 4–6, 1985 in New Delhi.

**Characters in bold face added by the author.

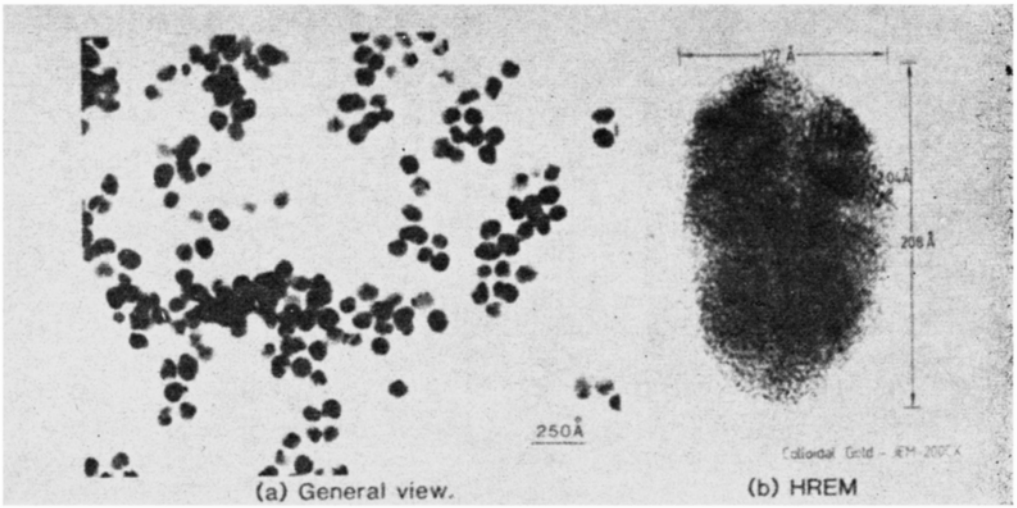

FIG 1 Colloidal gold particles prepared from a chlorauric acid solution reduced with sodium citrate. A High Resolution Electron Microscope picture of an individual gold particle is also shown.[2,46]

In the present work, an attempt is made to review certain aspects of the current state of investigations—both theoretical and experimental—of the electronic structure of metal particles which are neither quite microscopic nor macroscopic in nature. This short paper cannot hope to go into the details of the very rich and diverse properties of divided metals; rather, it will concentrate only on giving a representative outline of a variety of observations on divided-metal systems ranging from transition metal cluster compounds to colloidal metals. Throughout the bias will be towards studies carried out in the author's own laboratory.

An artist's impression of the problem at hand is given in Fig 2; this sets out the broad, global features while at the same time it attempts to provide a rough labelling or classification scheme for particles of different dimensions. These range from bulk, metallic solids through colloidal metals to metal cluster compounds (typically of the transition series). Clearly at each stage along the way (Fig 2), one has to consider not only the macroscopic topology of such divided or erstwhile metals, but also their microscopic structure ; *vis-a-vis*, the detailed nanostructure of the individual atomic constituents. Thus, particle diameters probably represent a reasonable coarse-grained parameter for arbitrarily classifying the various categories. In the case of the "atomic or molecular" transition metal cluster compounds[3] (e.g. $H_2Os_{10}C(Co)_{24}$), the cluster nuclearity is perhaps a more meaningful descriptive parameter which is certainly consistent with the atomic parentage of these species. We see, for example, in the cluster compound[4] $Au_{55}[P(C_6H_5)_3]_{12}Cl_6$ a gold cluster of an exceptional size for a molecular species. However, by the standards of colloidal gold science—in which one is typically dealing with Ca.

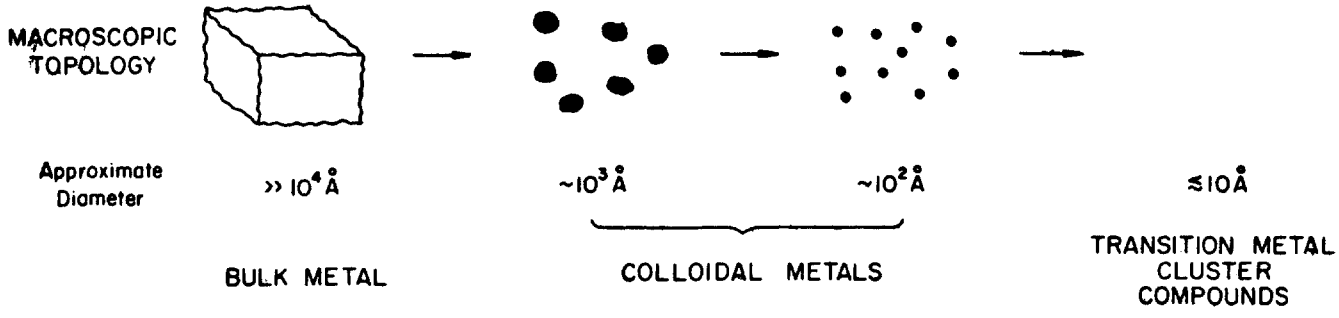

FIG 2 An artist's impression of the fragmentation or division of a bulk, metallic sample.

10^3–10^6 atoms in a fragment—such a particle is extremely small. But these are vexing questions of semantics which must necessarily arise in any discussion of materials which effectively provide the link between the macroscopic and microscopic regimes of matter.

One imagines that there must surely be a fundamental and qualitative difference between a piece of bulk, metallic gold and a relatively small collection of gold atoms (for example, in a colloidal particle) despite the fact that both consist of the same element. Our major problem, then, is the combined one of the synthesis of high-purity materials and the measurement of physical properties which reflect the successive fragmentation, or division, of a piece of bulk metal. Experimental techniques must yield formation on macroscopic morphology while at the same time probe both the nanostructure and electronic structure of Divided Metals.

Electrons in Divided Metals

In a recent elegant contribution, Perenboom, Wyder and Meier[5] outline the broad feature of the problem of Divided Metals, "... When the number of atoms contained in a grain of solid matter is steadily reduced, it is plausible that in the course of the process a stage is realized when the particle does not behave like a smaller copy of the corresponding bulk solid anymore." The last part of this statement....

> "...*when the particle does not behave like a smaller copy of the corresponding bulk solid anymore*,"

beautifully typifies the basic experimental and theoretical interest. I suggest, therefore, that two fundamental theoretical aspects need to be addressed:[6] The first concerns the possible electronic transition from metallic to insulating behaviour *within each grain* of solid matter. The second concerns the electronic and structural properties of small, isolated, but almost certainly "metallic," particles.

Localization, Charge Neutrality and the Metal-Insulator Transition

One inevitable consequence of the successive fragmentation of a piece of metal is the cessation of conducting behaviour within a small particle. A stringent lower limit for this transition would obviously be a cluster of only a few atoms. However, one clearly wishes to probe this Metal-to-Insulator Transition in more searching detail. Is there, for example, any similarity between the well-documented and prescribed descriptions for the Metal-Insulator Transition in what one might term "conventional" macroscopic systems (e.g. doped semiconductors)[7] and the proposed transition within a single particle in isolation? A schematic illustration of the possible situation in doped semiconductors and Divided Metals is given in Fig. 3. It is interesting to note that Sir Nevill Mott, in his celebrated paper[8] of 1961 entitled "The Transition to the Metallic State" alluded to just such a discussion. Concerning the proposed first order (discontinuous) nature of the transition in macroscopic systems, Mott noted[8] that "...*the sharp transition described here is only expected in an infinite lattice. It goes without saying that for a finite number of atoms there will be a gradual decrease in the weight of the ionized states in the wave*

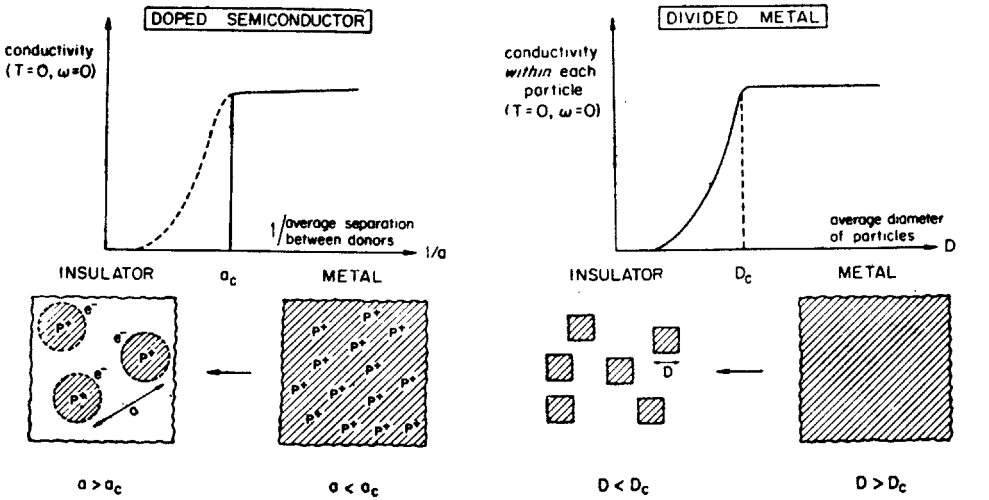

FIG 3 The Metal-Insulator transition in doped semiconductors and divided metals. A schematic representation which attempts to highlight the similarities and possible differences between the two situations at $\omega = 0$, $T = 0$ K.

function as the interatomic distance is increased or in other words, a gradual transition...." Fig. 3 attempts to illustrate the two situations. In the case of doped semiconductors, the transition from Metal to Insulator is effected by varying the donor (P°) atom concentration. Thus, the average separation (a) between donor states provides the demarcation between metallic ($a < a_c$, where a_c is the critical separation) and insulating ($a > a_c$) states in an (assumed) macroscopic assembly. The corresponding proposed transition within a Divided Metal would arise from a diminuition in the average diameter (D) of the individual particles. Here, the critical parameter may now be D, such that $D > D_c$ implies metallic status (for $\omega = 0$, T = 0), whereas $D < D_c$ implies insulating character. However, it may turn out that more detailed views of such a transition, involving a scaling theory for electrons in a disordered small particle, may also lead to a continuous conductivity transition in both representative systems.[9]

Wood and Ashcroft[10] make another interesting comparison between the two situations (Fig. 3). The Ioffe-Regel[11] criterion for the localization of electrons in the presence of scattering *i.e.*, the breakdown of the Boltzmann equation approach to conduction in conduction in a solid, is

$$k_F l \lesssim 2\pi, \qquad \ldots(1).$$

where l is the electron mean-free path and k_F is the Fermi wave-vector appropriate to the electron density. Thus, Ioffe and Regel[11] argued that since l is the distance over which the electron loses phase coherence, and the wavelength ($\lambda \sim k_F^{-1}$) is the distance over which the phase changes by 2π, it does not make sense to $\lambda \gg l$.

Wood and Ashcroft[10] suggest that if one crudely interprets l as a characteristic small-particle dimension (say, the diameter D), then the cessation of conducting behaviour in a small particle may be interpreted as a Metal-Insulator Transition of the Ioffe-Regel sort. For sodium metal, this transition should occur for particle dimensions below approximately 15Å.

In all of these considerations, however, the immediate and fundamental problem arises as to the "true" dimensions of a small particle. Here a knowledge of structural details at the nanometer level is essential (Fig. 1). That is, the particle itself may well be a collection of compact, finite sized metal-cluster subcomposites. For example, a particle of outside dimensions of say 1000Å may consist of isolated metal-particle clusters with characteristic radii 100Å ! It may also be the case—especially if these regions are not in close contact—that the electron mean free path (and corresponding scattering times, etc.) is dominated by the single particle dimension rather than the much larger particle dimension. This feature, noted recently by Curtin and Ashcroft,[12] will be discussed further in Sec. III. 4.

In discussing the interparticle interactions within these divided metals, another interesting analogy can be made with the Metal-Insulator Transition in nominally macroscopic systems (Fig. 4). It is generally assumed that the electron number in each small metallic particle is constant. This innovation, due originally to Kubo[13]

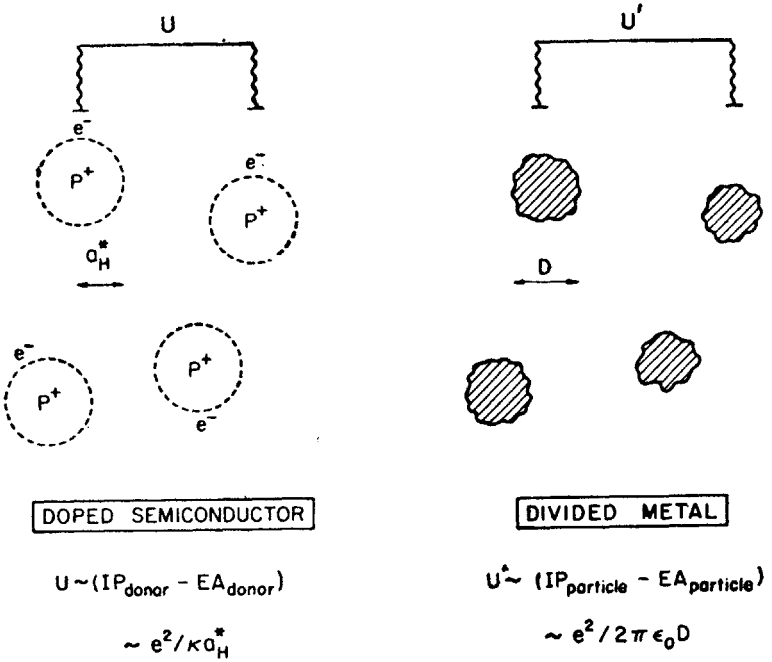

FIG 4 The metal-insulator transition in doped semiconductors and divided metals. A schematic representation of the Mott-Hubbard Correlation Energy, U, in the doped semiconductor, and the corresponding U' "charging energy" which maintains electrical neutrality in the Divided Metal.

has its "atomic" counterpart in the Mott-Hubbard correlation energy, U. The energy required to charge a metallic particle of diameter D with a charge in a vacuum is $U' \approx e^2/2\pi\epsilon_0 D$, where ϵ_0 is the vacuum permittivity. This charge can only originate from the surrounding medium which is at a temperature T. Therefore, when kT ($\sim 10^{-4}$ eV at 1 K, ~ 0.03 eV at 300k) is less than $e^2/2\pi\epsilon_0 D$ (~ 0.2eV for $D = 100$Å), the probability of electron transfer between particles is very small and therefore charge fluctuations are highly improbable. Note however, that such considerations tell us little about electron-electron correlation effects *within* a metal particle. One might imagine that for large metallic particles—in particular those in reasonable proximity to adjacent particles—this charging energy is small such that charge fluctuation may indeed occur. This situation is somewhat analagous to that found, for example, in doped semi-conductors and expanded metals *vis-a-vis*, the Mott-Hubbard correlation induced Metal-Insulator Transition.[9] The Mott-Hubbard correlation term U is, in the atomic limit, the different between the ionization energy (IP_{donor}) of the donor and the electron affinity of the donor (EA_{donor}) and $U \sim e^2/\kappa a_H^*$, where κ is an appropriate dielectric constant and a_H^* is the characteristic Bohr-orbit radius of the isolated donor state (Fig. 4).

Small Metallic Particles

A reasonable working definition might be a small particle which possesses a considerable and sufficient number of electrons such that the usual descriptions and methodology of solid state (metal) physics remain appropriate. Thus, one approach to the problem depicted in Fig. 2 revolves around the consequences of particle fragmentation within the framework of what one might term "bulk" solid state theory. Obviously, modifications due to the "smallness" of the system are added as a sort of perturbation. This approach would, presumably, be inappropriate for metal cluster compounds consisting of, say, 10 metal atoms, which one might deem to be approaching the atomic or molecular limit. However, as pointed out elsewhere,[5,6] it should give most useful and intuitive information when the particle dimensions are such that a realistic description is indeed one in terms of gradually reducing the size of the macroscopic, solid sample. In this spirit, a small metallic particle can then be considered as a solid with dimensions comparable to, or smaller than, some intrinsic length; for example, the electron mean-free path, the wavelength of light, etc.

It is important to reiterate the view[5,6] that a very clear distinction has to be made between the electronic energy-level structure of the full thermodynamic, many-particle system, and the electronic structure of a *single* quantum-mechanical particle, both in a finite volume.

In a bulk metal, the electron energy levels form a continuous set which are generally interpreted as being independent of any particular boundary conditions imposed on the electron wave-function. This standard picture must clearly be modified for metallic particles of dimensions smaller than, say, 10^3Å. Thus, the imposed truncation of the one-electron wave-function has two effects on the electronic properties of the particle.[5] The first is a surface effect. The fraction of surface atoms

increases rapidly as the particle diameter decreases. For example, Fig. 5 shows the effective fraction of surface atoms for sodium particles of various diameters. Thus, for sodium particles of less than 100Å diameter, at least 10 per cent of the constituent atoms are located on the particle surface.

The second effect results from the imposed discreteness of the electronic energy levels due to the smallness of the system. For a particle containing N atoms, the spacing (Δ) of adjacent energy levels will be of the order* of E_F/N, where E_F is the Fermi energy appropriate to the bulk metal. It is perhaps obvious (especially in hindsight), as was realized many years ago, that interesting effects should occur if the average value of Δ for a particle becomes comparable to, or greater than, some important characteristic energy. For example, when Δ is larger than the thermal energy, kT, the electronic Zeeman energy ($g_e\mu_B H$), the energy of incident radiation ($\hbar\omega$) etc.

The resulting consequences are generally termed quantum-size effects. In Fig. 5, we also show the average one-electron energy level gap (calculated for

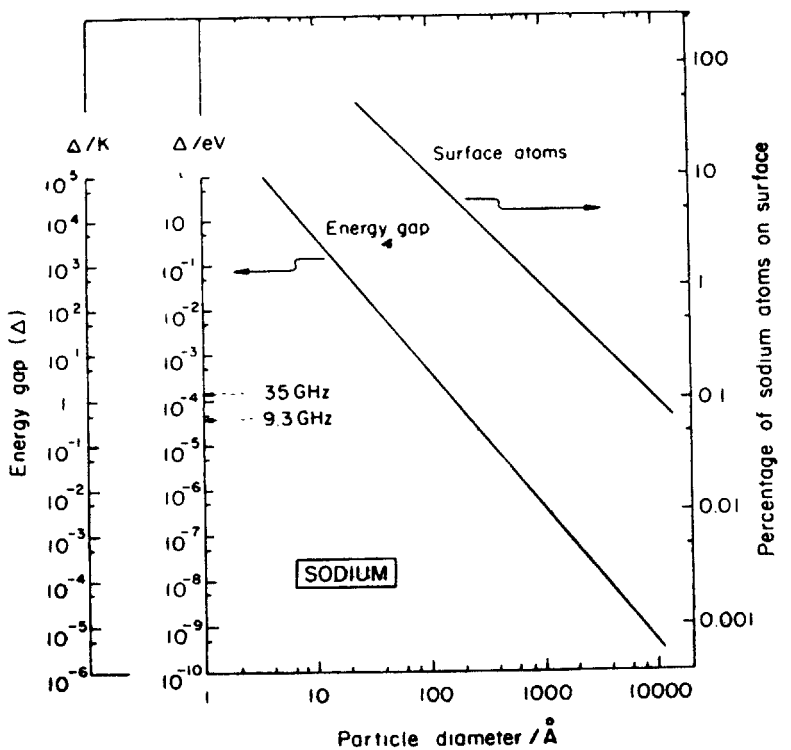

FIG 5 The fragmentation of bulk sodium metal. A plot of the average energy level separation as a function of the particle diameter D. The figure also shows the calculated surface fraction of atoms in a particle as a function of particle diameter.

*See also ref. 10 for a discussion of this point.

sodium using $\Delta \sim E_F/N$) as a function of particle diameter, with Δ parameterized in both eV and K. Therefore, one anticipates size effects to be important, for example, when $\Delta \gtrsim kT$, so that for a Na particle with $D \sim 100$Å, this condition would be satisfied below approx. 5 K; for a particle with $D \sim 30$Å the corresponding temperature is 300 K. We also indicate in Fig. 5, the typical values of the electron spin Zeeman energies at both X-and Q-band operating frequencies. It seems clear, therefore, that for particles with diameters below ca. 200–300Å, magnetic susceptibility, magnetic resonance and many other properties (e.g. optical) may be greatly affected by this energy level structure. In addition, it is widely supposed[13,14] that the dynamic response of both electrons and nuclei in small metallic particles at a frequency ω such that $\Delta \gtrsim \hbar\omega$ may indeed be dramatically different from those of bulk metals.

While we obviously have many suggestions from theory, the answers to many of the questions raised earlier will always be based on experimental facts. The aim of experimentalists in this area is to provide laboratory conditions whereby a variety of cluster properties can be observed from high-purity, stable particles with a very narrow size-distribution. Therefore, the rate-determining step to major theoretical innovation in this area relies heavily–one might even say completely-on the synthesis, characterisation and investigation of high-purity divided metal samples. In the following sections we present a very brief overview of a variety of experimental systems currently under investigation. Here, the emphasis is on solid state materials, and a strong leaning towards the study of these systems *via* magnetism, magnetic resonance and electron microscopy.

Probing the Electronic Structure of Divided Metals

In order to handle and study Divided Metals they must clearly be prevented from accidentally interacting with themselves or any other substance which might perturb their properties. In this section we outline just a few methods of[15] realizing this aim.

Phonon Softening in Metal Particles

The electrical resistivity of an ideal (bulk) metal has been calculated by Ziman[16]

$$\rho = C\,\frac{T}{\Theta_D}\int_0^{\Theta_D/T}\frac{x^5}{(e^x-1)(1-e^{-x})}\,dx = C\,\frac{T}{\Theta_D^2}\,\mathcal{G}(\Theta_D/T) \qquad \ldots(2)$$

This is the well known Bloch-Grüneisen equation defining the Grüneisen function[17] $\mathcal{G}(\Theta_D/T)$, where C is a constant depending on the metal and Θ_D is the Debye temperature. This describes the electron-phonon scattering process which causes transitions between k-states and hence gives rise to electrical resistivity in the bulk metal. It is therefore possible to define a reduced resistivity $\rho_T/\rho_{T\Theta_D}$ given by[17] $\rho_T/\rho_{T\Theta_D} = 1.056\,(T/\Theta_D)\,\mathcal{G}(\Theta_D/T)$ where ρ_T, $\rho_{T\Theta_D}$ are, respectively, the ideal

resistivities at temperatures T and Θ_D. Fig. 6 shows a plot of the experimentally measured electrical resistivity of bulk potassium metal (filled squares) and the theoretically predicted variation of $\rho_T/\rho_{T\Theta_D}$ *via* the Bloch-Grüneisen relation. As one can see there is excellent agreement between the observed and theoretical resistivity behaviour. One might ask, therefore, "How does this description of the electron-phonon interaction survive as we successively fragment a bulk metal into small particles?" (Fig. 2). To investigate this, we consider direct conductivity measurements on fine particles of Al and Ag, as well as conduction electron spin resonance (c.e.s.r.) measurements on the alkali metal colloids.

We turn first to the measurements on Al and Ag.

An alternative representation of resistivity data at various temperatures involves treating the Debye temperature Θ_D as a floating (temperature-dependent) parameter. In this way, Θ_D can be derived from resistivity measurements by fitting the experimental data to the Bloch-Grüneisen function. Ohshima *et al*[18,19] have reported resistivity measurements on Al and Ag particles with diameters down to 100Å. Their data are reproduced in Fig. 7 with the appropriate values of Θ_D.

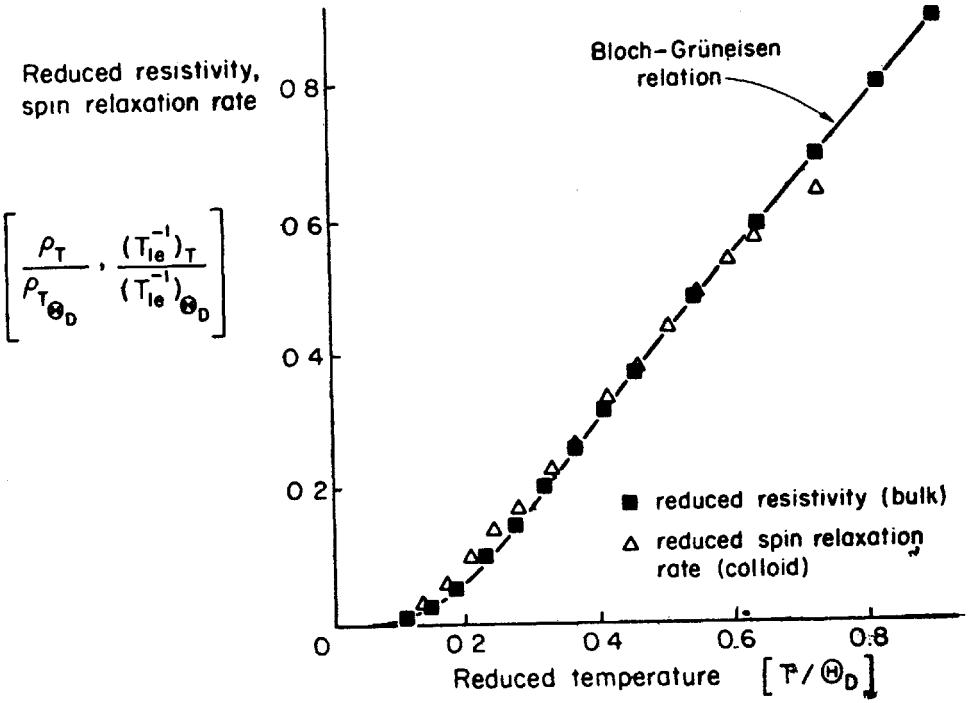

FIG 6 The duality of electron spin and resistivity scattering in bulk and colloidal potassium. A plot of the experimental reduced electrical resistivities and spin-relaxation rates against reduced temperature for potassium. The solid line is the theoretical Bloch-Grüneisen relation (eq. 2).

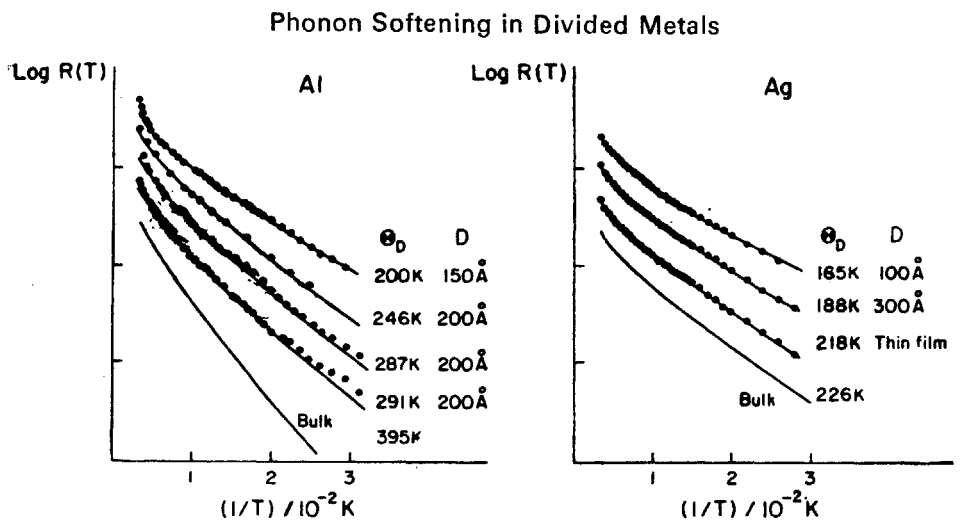

FIG 7 Phonon softening in small particle samples of Al and Ag. The plot shows the experimental resistance of the samples as a function of T^{-1}, for various particle sizes (D). The derived (eq. 2) Debye temperatures are also shown.[18,19]

from experiment; in each case, the solid line is the theoretical resistivity variation (from q. 2) using the suitable Debye temperature (shown also).

This lowering of the Debye temperature or "phonon-softening" in small metallic particles has been observed in a variety of systems. It has been suggested that the phonon spectra of a small particle is modified from that of the bulk metal in two ways; a low frequency cut-off due to the restriction of a finite particle size and a general lowering of phonon frequencies due to the weaker vibrational potential of the surface atoms.

Another technique for directly probing the electron-phonon interaction is c.e.s.r.; recent studies on alkali metal colloids[20,21]—respectively large with $D \sim$ 1000–1500Å—rely on the apparent duality of both electron-phonon and spin-phonon interactions in metals.

Elliott's[22] relation between the phonon spin-lattice relaxation rate T_{1e}^{-1} and the corresponding resistivity relaxation rate τ_R^{-1} (which is proportional to the electrical resistivity) is

$$T_{1e}^{-1} = T_{2e}^{-1} = \alpha\,(\Delta g)^2\,\tau_R^{-1}, \qquad \ldots (3)$$

where α is a numerical constant and Δg is the deviation of the observed electron g-factor from the free spin value (2.00231).

It was suggested by Yafet[23] that T_{1e}^{-1} may also be described by the Bloch-Grüneisen function (eq. 2) with a different constant C which now involves its matrix

elements of the spin-orbit coupling operator between spin-up and spin-down Bloch wave functions. Yafet's[23] detailed calculations showed $T_{1e}^{-1} \propto T^5$ at low temperatures, changing to $T_{1e}^{-1} \propto T$ at high temperatures. This prediction for the c.e.s.r. case is observed for the corresponding temperature dependence of the electrical resistivity in a wide range of metals. To illustrate this duality in both electron spin and resistivity scattering processes[21] in the alkali metals and colloids, we show in Fig. 8 the intrinsic electron spin relaxation rates in sodium, potassium and rubidium colloids ($D \gtrsim 10^3$Å) as well as the corresponding electrical resistivities of the bulk metals. Note also that c.e.s.r. data for bulk potassium are also included in Fig. 8, and these are in agreement with the form of the colloidal particle results. We can see, therefore, that there are indeed clear parallels between the temperature dependence of the electrical resistivity and spin relaxation rates for these three metals. From eq. 2 it is also possible to define a reduced (intrinsic) spin relaxation rate $(T_{1e}^{-1})_T/(T_{1e}^{-1})_{\Theta_D}$, in analogy to the reduced resistivity (Fig. 6), where the subscripts denoted a temperature T and the Debye temperature, respectively. Since Δg is temperature independent, eq. 2 indicates that the similarly defined reduced spin relaxation rate should be described by the same Bloch-Grüneisen function. In Fig. 6, these quantities are plotted both from resistivity and c.e.s.r. measurements on potassium (bulk and colloidal samples) along with the function defined by eq. 2 assuming a Debye temperature of 110 K.

One can adopt a similar procedure to that outlined for resistivity measurements for processing the electron spin relaxation data; namely, treating the Debye temperature

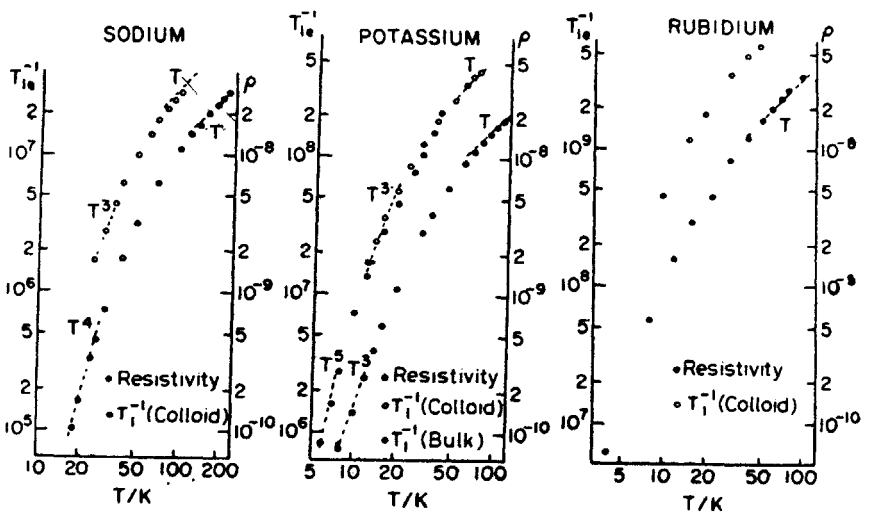

FIG 8 The temperature dependence of the intrinsic electron spin-spin relaxation rates as a function of temperature for sodium, potassium, rubidium and caesium colloids. Also included is the corresponding temperature dependence of the ideal electrical resistivities for these metals. In all cases the temperature exponent is indicated (Ref. 21).

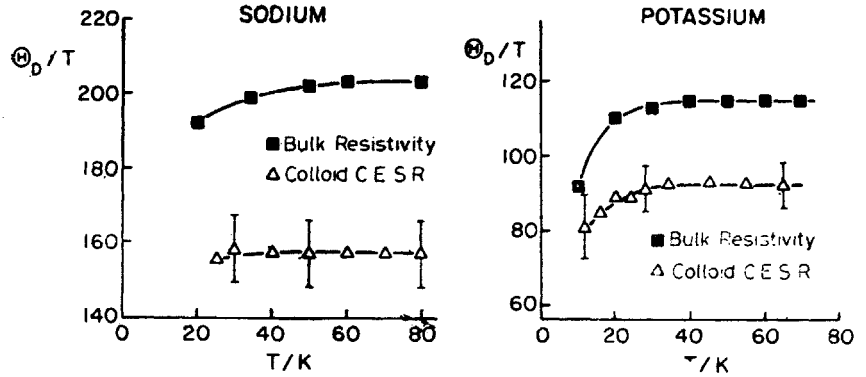

FIG 9 Experimental Debye temperatures for sodium and potassium derived from bulk electrical resistivity and colloidal c.e.s.r. measurements. Note the decrease in Θ_D for the colloidal particles (Ref. 21).

as a temperature-dependent parameter and evaluating the characteristic temperatures from the resistivity and spin-relaxation data, respectively. The results for sodium and potassium are shown in Fig. 9. Once again, one sees a reduction in the Debye temperature or "phonon softening" in these small metallic particles. It is interesting to note that this reduction is Θ_D for both the alkali samples,[20,21] and those of Al and Ag[18,19] (Fig. 7) appears to be a smooth function of D, for diameters down to 150Å (in the case of Al) and 100Å (in the case of Ag). However, we once again raise the question of the microscopic nature of the Al, Ag samples; namely, the considerable difficulties of actually measuring electrical resistivities for very small samples which may well be more representative of a percolation problem.[24] Similar problems may also pervade the c.e.s.r. studies on quenched metal solutions, but it is interesting to note that there does appear to be a rather impressive adherence to the Bloch-Grüneisen function for particle sizes down to approximately 50Å.[25,26] This suggests that only minor changes occur in the gross details of the lattice (phonon) spectrum of these divided metals for dimensions down to the onset of the quantum size-effect regime.

Ionic and Metallic Species in Zeolites and Vycor

A large number of inorganic materials contain regular cavities or vacancies forming networks or parallel channels. In zeolites the size of the cavities is typically in the range from 2–12Å. Within these cavities metal clusters and particles can be sorbed or produced *in situ*. In addition, the availability of several types of zeolites means that different three-dimensional arrangements of cavities can be investigated for preparing and stabilizing small metallic particles. In recent work[27,28] we have concentrated on faujasitic zeolites in their sodium, potassium and rubidium-cation exchanged form. A representation of the structure of faujasitic zeolites is given in Fig. 10.

The polyhedron with 14 vertices (tetrakaidecahedron) in Fig. 10 is known as the sodalite or β-cage and is the principal building block of the 3 structures shown

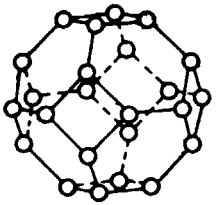

Truncated octahedron

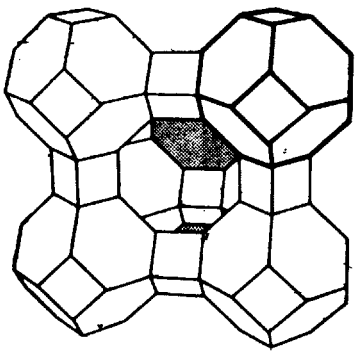

Zeolite A

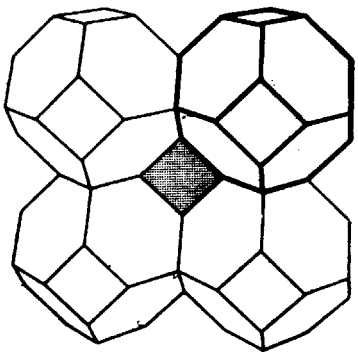

Sodalite

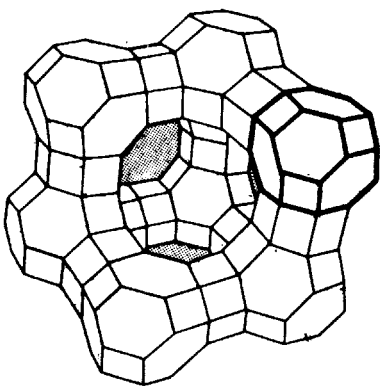

Faujasite (zeolites X and Y)

FIG 10 The sodalite cage and the structure of zeolites belonging to the faujasite family. The framework oxygen atoms and exchangeable cations are not shown.

in the figure. Only one type of cavity occurs in sodalite, with a diameter of 6.5Å and accessed through small 6-membered pores some 2.2Å in diameter. There are approximately 6 alkali metal cations in each sodalite cage.

Zeolite A is a synthetic mineral with no natural counterpart. The sodalite cages are connected by double four-membered rings, forming an interconnected set of larger cavities within the material known as α-cages with a diameter of 11.5Å and accessed through eight-membered pores 4.2Å in diameter. There is one α-cage for every sodalite cage and 12 alkali-metal cations are distributed between them.

Zeolites *X* and *Y* are the synthetic counterparts of the naturally occurring mineral faujasite. Here the sodalite cages are connected by double six-membered rings forming an interconnected set of even larger cavities within the material known as α-cages (or supercages) with a diameter or 12.5Å and accessed through 12-membered pores 7.5Å in diameter.

Two distinct species can be formed following the reaction of, for example, Na^+-exchanged Zeolite *Y* with the vapour of sodium, potassium, rubidium or caesium metals.[27,28] The relative amount of the two species can be changed by varying the concentration of the alkali vapour.

Ionic Clusters in Zeolites : The exposure of Na^+-Zeolite *Y* to a low concentration of alkali vapour results in brightly coloured samples whose electron spin resonance (e.s.r.) spectra are characteristic of the ionic cluster, Na_4^{3+}. This species consists of an unpaired electron interacting with 4 equivalent sodium nuclei (^{23}Na, $I = 3/2$, 100 per cent abundance). Similarly, the reaction of K^+-Zeolite Y with alkali vapour gives rise to the correspoding potassium species K_4^{3+}. The e.s.r. results[27,28] are summarized in Fig. 11. Interestingly, no e.s.r. signals indicative of Rb_4^{3+} clusters were ever found in corresponding reaction with Rb^+-exchanged Zeolite *Y*. Thus, the reactions of Na^+-and K^+-exchanged Zeolite with low concentrations of alkali metal vapour can therefore be written (in a manner formally akin to the formation of an F-centre) as

$$4Na^+ + M^0 \rightarrow Na_4^{3+} + M^+$$

and

$$4K^+ + M^0 \rightarrow K_4^{3+} + M^+,$$

where M^0 represents the vapour of sodium, potassium or rubidium. The available evidence to data suggests that the ionic M_4^{3+} clusters are almost certainly accommodated within the sodalite cages (β cages) in the structure, as shown in Fig. 12. We believe that the rubidium ionic cluster Rb_4^{3+} either does not form at all, as it is unstable to disproportionation with respect to small metallic particles. Specifically, computer simulations (shown in Fig. 13) suggest that geometrical/spatial considerations may well form the most important feature in inhibiting Rb_4^{3+} formation in the sodalite cage. Consistent with this, we note the difficulty in routinely exchanging Na^+ cations in Zeolite-*Y* for the corresponding Rb^+ cations.

Metallic Clusters in Zeolites : Exposure of Zeolite samples to a high concentration of alkali vapour results in dark-coloured (generally blue/black) samples with an e.s.r. signal characteristic of small metallic particles. These may also be initially located within the sodalite cages, but at high (metal) doping levels we have assumed that the large "metallic" clusters are accommodated within the α-cages (Fig. 10).

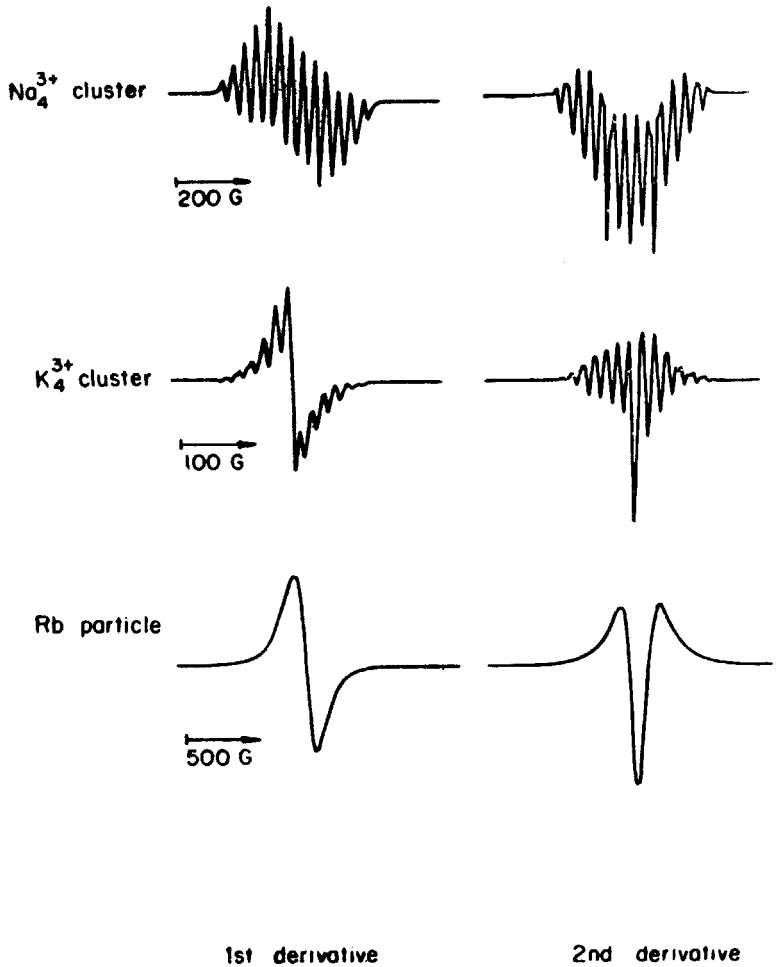

FIG 11 Esr spectra of alkali-doped zeolite Y samples, showing both 1st and 2nd derivative spectra. Here we show the Na_4^{3+} cluster in zeolite $Na^+ - Y$, the K_4^{3+} cluster in zeolite $K^+ - Y$ and the rubidium metallic cluster observed in $Rb^+ - Y$ zeolite after exposure to rubidium vapour.[37]

There is, as yet, no structural data on these metal-loaded Zeolites to confirm or refute this suggestion.

As we have noted in Sec. II. 2, and III, 1 the electron spin relaxation rate in metal particles depends critically upon their size. If the particles are sufficiently large such that $\Delta \ll g_e \mu_B H$ (Fig. 5), the electron-spin surface scattering rate (and hence the e.s.r. line width) should vary inversely with the diameter of the particles. Here, spin-phonon scattering closely follows the Bloch-Grüneisen law (Figs. 6, 8) and the magnetic susceptibility follows a Pauli-type, temperature-independent paramagnetism. Conversely, if $\Delta \gtrsim g_e \mu_B H$, then both surface scattering and phonon-scattering mechanisms are quenched. Thus, relatively narrow e.s.r. signals can be

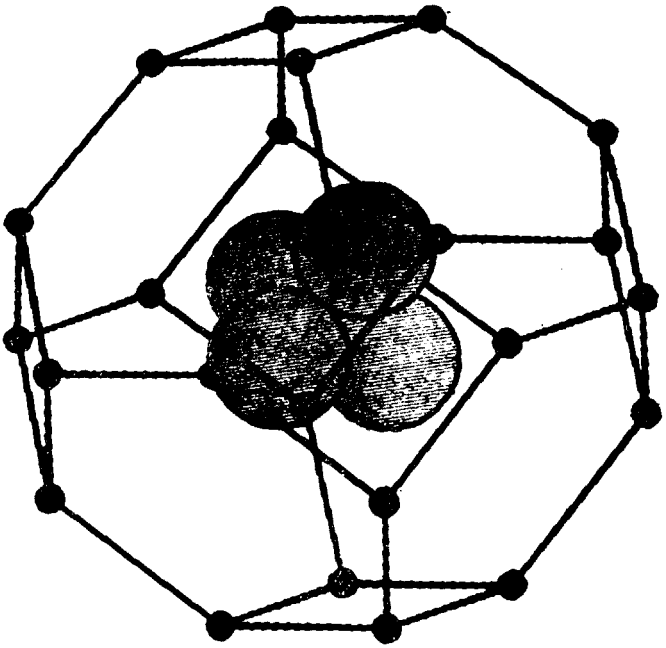

FIG 12 An illustration of a sodalite cage containing a Na_4^{3+} cluster of (presumed) tetrahedral geometry.[27]

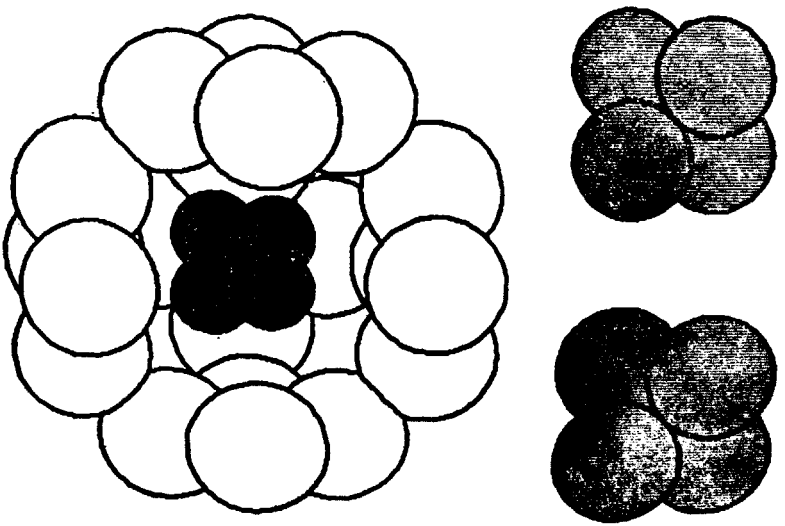

FIG 13 A scale view of a Na_4^{3+} cluster within a sodalite cage. Top right; a K_4^{3+} cluster drawn to scale. Bottom right; a hypothetical Rb_4^{3+} cluster.[27]

observed at comparatively high temperatures ($T/\Theta_D \gtrsim 0.5$–1.0), even in the heavier metals[29] for which spin-orbit coupling constants are very large. In addition, the

paramagnetic susceptibility of the particles is expected to follow a Curie-type variation with temperature.

This quantum size-effect was predicted to occur in sodium particles smaller than 100Å, which is certainly much larger than the particles postulated to be in the Zeolite cavities. Therefore, it has been suggested that the "metallic" e.s.r. signals observed in the concentrated samples are characteristic of small particles of alkali metal located within the Zeolite cavities. As expected, the electronic *g*-factors of the metallic particles (Table I) highlight the very great importance of the spin-orbit interaction in the heavier metals. Most striking, the particles of the heavier metals K, Rb and Cs appear to be small enough to quench the usual rapid spin-relaxation mechanism operative in bulk samples of these elements. A possible explanation relies on the relative size of the atoms; more sodium atoms can obviously fit into the Zeolite cavities than can rubidium atoms. Thus the sodium metallic particles possibly contain more atoms than their rubidium counterparts and hence have properties more similar to the large, colloidal samples discussed earlier (III. 1). Our recent Faraday susceptibility experiments[30] reveal that heavily loaded sodium samples (for which the "small metallic particle" e.s.r. was observed) show a paramagnetic susceptibility behaviour which follows a Curie-type variation with temperature. These metal-loaded Zeolites may therefore be ideal materials to study the unsual electronic properties of small metallic particles.

TABLE I

Electronic g-values for alkali metal particles in Zeolites and Vycor

Metal	Particles in Vycor[a]	Particles in Zeolites[b]	Bulk Metal
Sodium	1.996 ± 0.001	1.9997	2.0015
Potassium	1.999 ± 0.001	1.9978	1.9997
Rubidium	1.988 ± 0.001	1.989	1.9984
Caesium	2.010 ± 0.03	—	2.013

[a] ref. 31

[b] ref. 28

Similarly, we have recently investigated the use of porous "Vycor" glass as a supporting matrix for silver and alkali metal particles. This glass is perforated with channels between 40 and 70Å in diameter, and thus contain larger cavities than in Zeolites. We have reported a variety of methods of preparing Vycor-supported silver particles, as well as alkali metal colloids supported by Vycor glass. The *g*-values for one sample each of sodium, potassium, rubidium and caesium are given in Table I. The *g*-values in Table I are indeed very similar to those of metal particles in Zeolite-*Y* and in some cases differ significantly from the bulk values (which are also given for comparison).

Transition Metal Cluster Compounds

There exists a wealth of well characterized metal-cluster complexes[3] which are ideal candidates for the study, amongst other things, of the genesis of "metallic" properties from the molecular regime.[32] These clusters generally have a poly-nuclear, metal-metal bonded core and a tightly bound outer ligand covering of, for example, CO molecules. Thus, the cluster carbonyls of various transition elements have been shown by X-ray crystallography to exhibit many different geometries. These compounds represent cluster fragments effectively isolated from adjacent cluster units by inert sheaths of carbonyl ligands. In Fig. 14, we show a representation of the typical metal atom geometries in transition-metal carbonyl clusters.[32]

A recent study of magnetism in the cluster compounds of osmium begins to shed light on the evolution of certain aspects of what one might term "metallic" behaviour. Johnson *et al.*[32] report measurements of the magnetic susceptibilities of a series of cluster compounds of osmium (Fig. 15) over the temperature range 1.5–300 K. With the exception of the hydrido cluster $H_2Os_{10}C(CO)_{24}$ the magnetic susceptibilities of the entire series of clusters were rigorously temperature independent down to 1.5 K. It is possible to estimate from these data the excess paramagnetic molecular susceptibilities after allowing for the ion-core and ligand contributions.[32] The observed susceptibilities (Fig. 15) are most naturally interpreted as arising from a Van Vleck paramagnetic contribution to the susceptibility. This modification arises from the modification of the cluster wavefunction caused by the external magnetic field. The modified wave function is described by the admixture of excited states in which electrons are 'promoted' from occupied bonding orbitals to the first unoccupied (antibonding) levels. The increase in this Van Vleck paramagnetism (Fig. 16) suggests that the charatceristic energy gap separating filled from vacant orbitals decreases with increasing cluster size. Note also in Fig. 15 that the high nuclearity cluster $H_2Os_{10}C(CO)_{24}$ behaves in a rather different fashion, showing a marked temperature dependence in the susceptibility at low temperatures. Obviously, paramagnetic impurities can play havoc with any interpretation of genuine (i.e. intrinsic) paramagnetism. In the study of osmium cluster carbonyl, strenuous efforts were made to eliminate possible paramagnetic contaminants. In addition, recent studies of the magnetic behaviour of high nuclearity platinum clusters[33] and "Cherry" crystallites[34] [e.g. $Ni_{38}Pt_6(CO)_{48}H_{6-n}]^{n-}$ ($n = 5,4$) ions show unusual magnetic behaviour.

It is interesting to question theoretically how the Van Vleck paramagnetism is modified as the characteristic HOMO-LUMO energy gap changes.[32,35] We take the molecular cluster as having no magnetic moment in the ground state (as required by most bonding models). Suppose there is a non-diagonal matrix element $(n|\mu_z|0)$ of the magnetic moment operator, connecting the ground state D with the excited state n of energy $\Delta = E_n - E_0$ above the ground state. Then by standard perturbation theory we see that the wave function of the ground state in a small field ($\mu_z H \ll \Delta$) becomes[35]

$$\psi_0 = \psi_0 + \frac{(Hn \mid \mu_z \mid O)}{\Delta} \psi_n$$

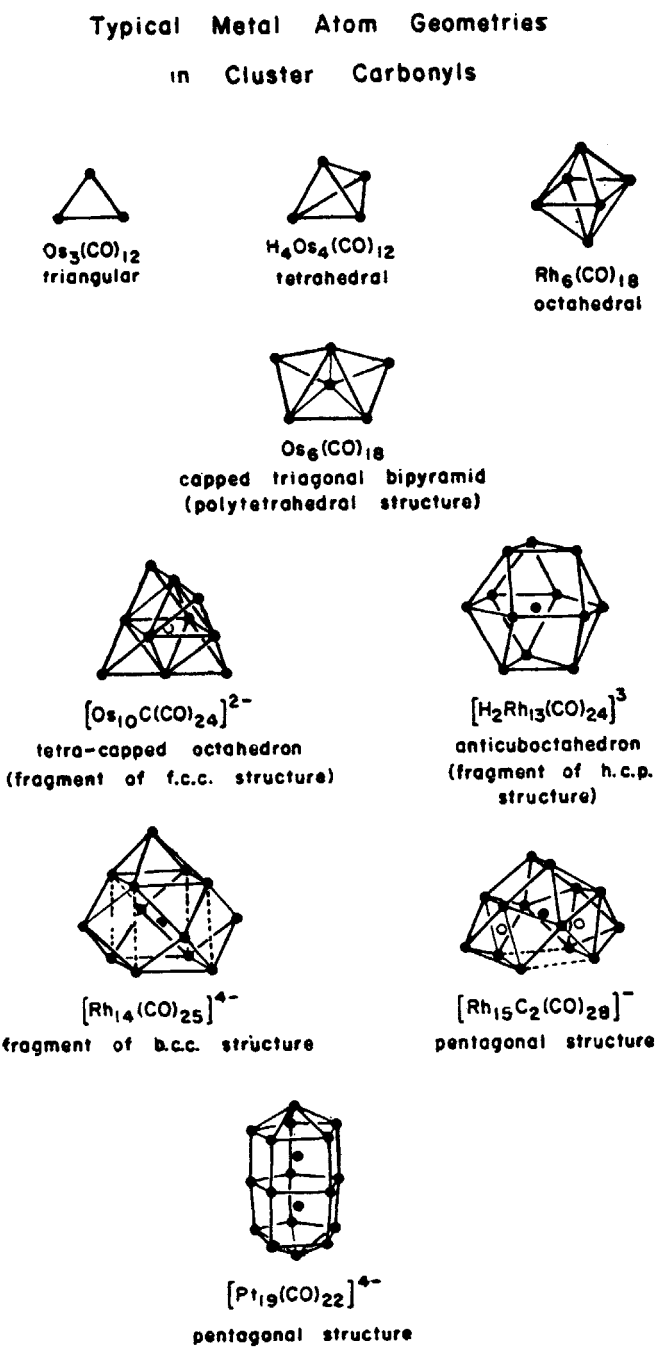

FIG 14 A representation of the typical metal atom geometries in transition metal carbonyl clusters. For clarity, the carbonyl ligands have been omitted. The open circles denote interstitial C atoms in the cluster.[32]

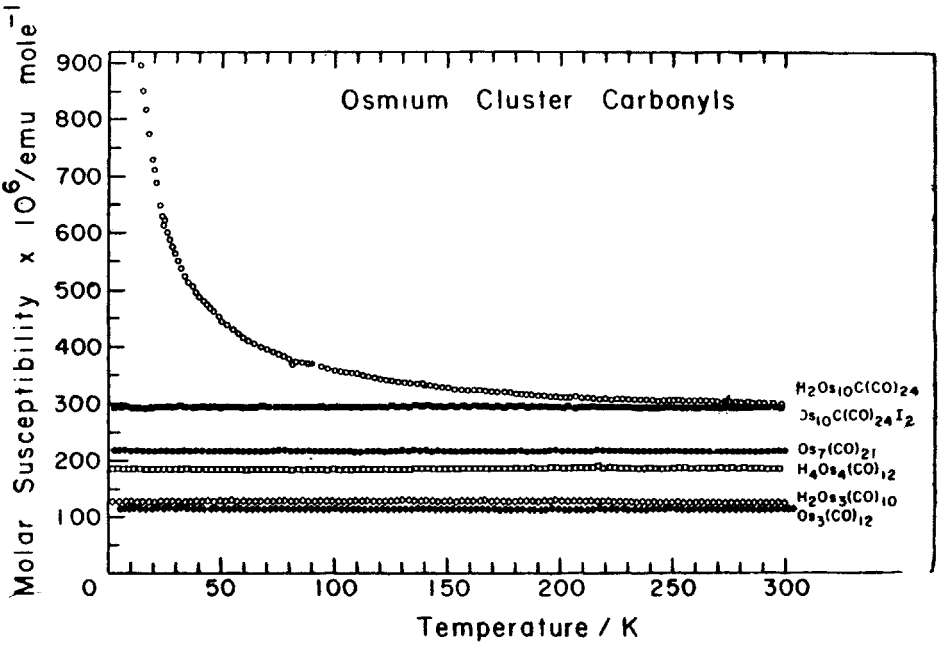

FIG 15 The excess molecular susceptibility in osmium cluster carbonyls.

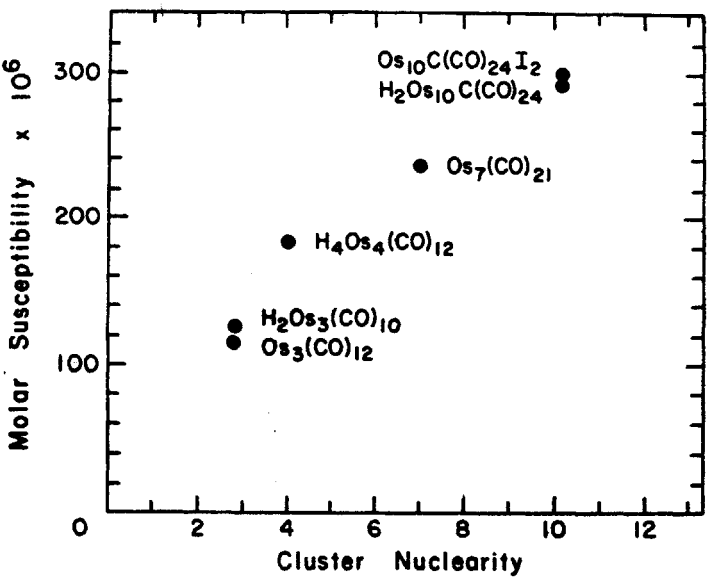

FIG 16 Paramagnetism in osmium cluster carbonyls; the variation of the high temperature (298 K) excess molecular susceptibility for osmium cluster compounds of increasing nuclearity.[32]

and the wavefunction of the excited state becomes

$$\psi_n' = \psi_n - \frac{H(\mathrm{O} \mid \mu_z \mid n)}{\Delta} \psi_0$$

The upper state then has a moment

$$-2H \mid (n \mid \mu_z \mid \mathrm{O}) \mid ^2/\Delta.$$

The total (induced) magnetic moment in the system is now

$$\mu_{total} = \frac{(n \mid \mu_z \mid \mathrm{O}) \{1 - (\exp(-\Delta/kT))\}}{1 + (\exp(-\Delta/kT))}$$

Consider two limiting cases :

(a) $\Delta \ll kT$

The surplus population in the ground state is approximately equal to $N\Delta/2kT$, where N is the Avogadro number, which gives for the suceptibility,

$$\chi = \frac{N \mid (n \mid \mu_z \mid 0) \mid ^2}{kT}.$$

This contribution is of the usual Curie form, although the mechanism of magnetization here is through polarization of the states of the system, whereas with "free" spins the mechanism of magnetization is the redistribution of ions among the states.

(b) $\Delta \gg kT$

The population now is almost nearly all in the ground state, so that the susceptibility is, summed over all suitable states n,

$$\chi = 2N \sum_n \frac{\mid (n \mid \mu_z \mid 0) \mid ^2}{E_n - E_0}$$

and independent of temperature.

Thus, the observed (Fig. 16) increase in the Van Vleck paramagnetism in the larger clusters may in part, be associated with the gradual diminuition in $E_n - E_0$.

Finally, it is interesting to speculate[35] on the most noticeable lack of nuclear magnetic resonance (nmr) observations on the large platinum (and other) molecular clusters.[34] The possible occurrence of such a large (induced) paramagnetism will give rise to a concomitant paramagnetic contribution to the n.m.r. chemical shift.[32] This, for nuclei in a fairly low symmetry environment, relaxation via chemical shift anisotropy may well be extremely efficient in these large clusters, leading to excessive n.m.r. line broadening.

Colloidal Metals Revisited

This paper was begun with a brief reference to Faraday's remarkable observations[1] on the nature of colloidal gold as a Divided Metal. In this final section, I

FIG 17 A high resolution electron microscope photograph of an individual gold particle.[2]

will give a brief mention of more recent studies on colloidal gold[2,36]. My aim here is to show how key experiments on this old and venerable area of Chemistry are now possible given the considerable power and utility of High Resolution Electron Microscopy.[37,38]

Colloid Chemistry is one of the oldest branches of ihe chemical sciences, once thought by many to be past its zenith. Within this last decade, however, there has been a powerful renaissance of interest in the subject, particularly as regards the chemical and physical properties of colloidal aggregates of small metal particles. These colloidal particles represent a domain of matter intermediate between the bulk, macroscopic metallic state and the microscopic world of atomic and molecular clusters (Fig. 2).

Fig. 17 shows a high resolution micrograph of a colloidal gold particle of diameter 50–55Å. Here the atomic planes in the constituent twinning particles may possibly be now identified.[2,36] Such investigations will, I feel, lead to a detailed microscopic picture of the composite topology of colloidal particles. Our initial work suggests that the colloidal particle is a collection of intergrown subcomposites. In these systems, the electronic scattering time τ_R may be dominated by a scattering length determined by the single, subcomposite dimension, rather than by the much larger colloidal dimension. This "cluster" composite view has recently been

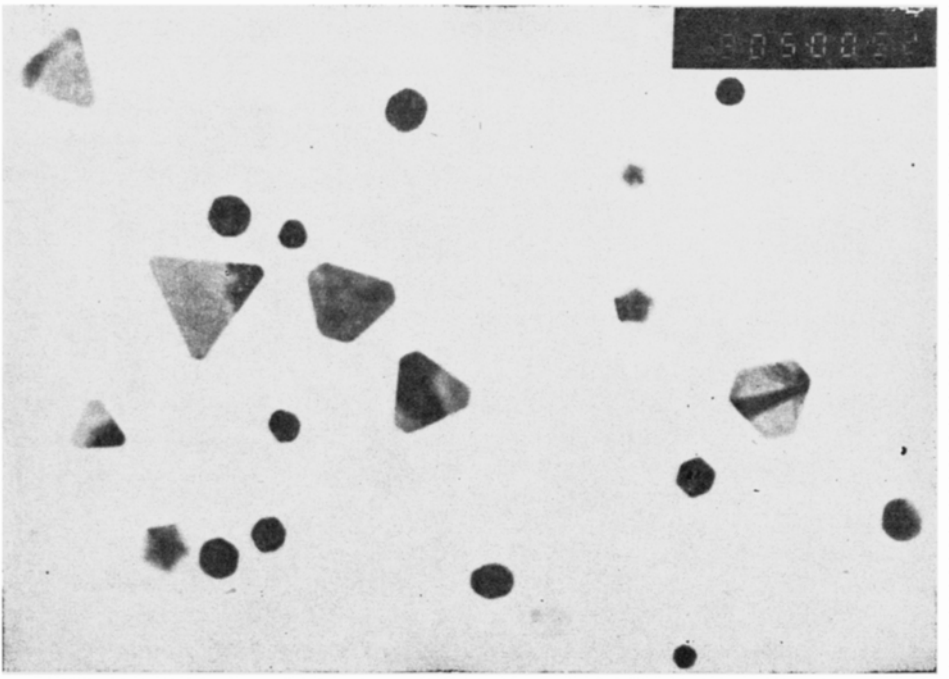

FIG 18(*a*) Transmission electron microscope photographs of (*a*) gold "trigons".

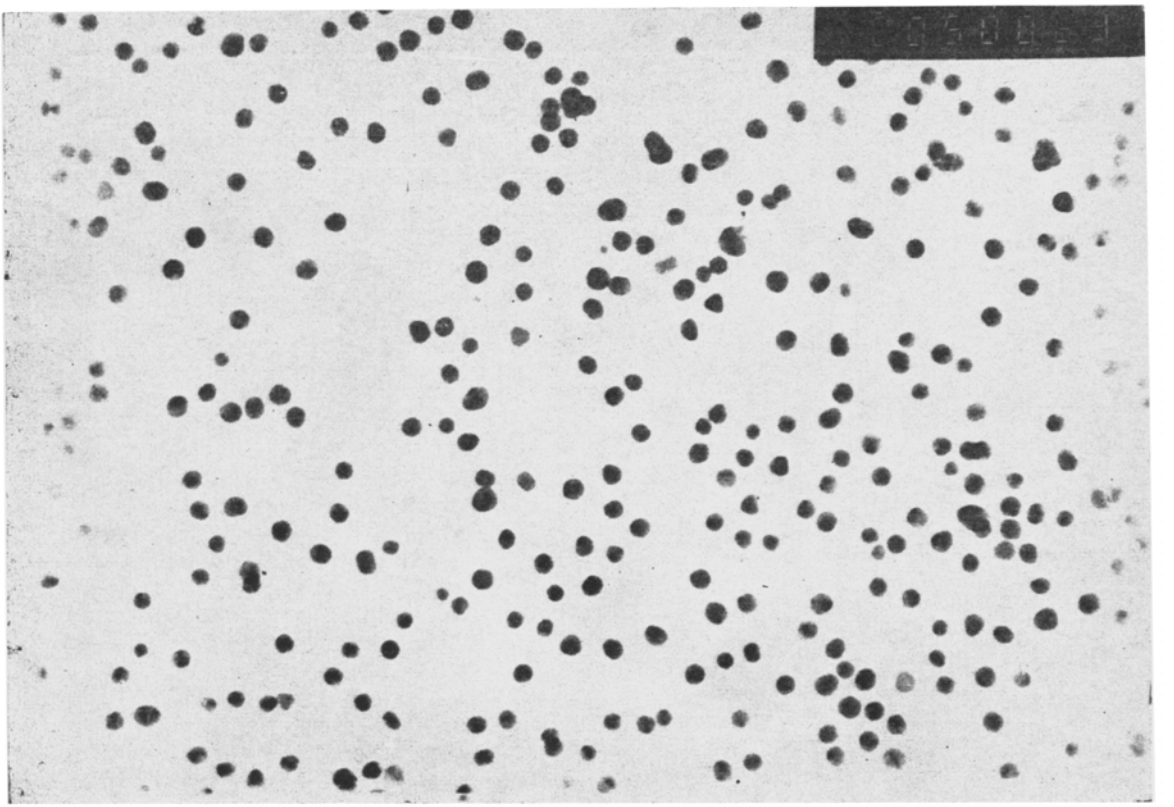

FIG. 18(*b*) Spherical particles.

advanced by Curtin and Ashcroft[12] to account for far-infrared absorption coefficients in small particle systems. Colloidal gold can also be formed as pentagonal bipyramidal particles. Fig. 18 shows gold sols prepared in our laboratory both by citric acid (platelets) and sodium citrate (spherical particles) routes. The conditions for both preparations are identical (the same volume of 1 per cent solution of each reducing agent added). One's hope is ultimately to develop morphology-selective preparations of small gold particles.

One must conclude that, just as in Faraday's day, attempts to characterize and explain the physico-chemical properties of colloidal, divided metals still pose a strong challenge to experimenter and theoretician alike.

CONCLUSION

The title 'Divided Metals' is in some ways a misnomer; if the individual grain of matter is sufficiently divided, one anticipates a transition to insulating behaviour ! (see Fig. 3). However, I hope to have illustrated that a 'gedanken experiment'—as popularized in Fig. 2 may indeed be a reflection of genuine experimental systems

which straddle the demarcation between the macroscopic and microscopic regimes of matter. I have noted that a reduction in the number of atoms contained within a grain of solid metal may lead to interesting changes in electronic properties due to the appearance of a respectable energy gap in an (assumed) continuum of levels. The further fragmentation of an erstwhile metal particle may lead to an even more drastic modification; namely, the cessation of metallic conductivity wilhin the grain of matter. The precise experimental conditions for effecting the transformations (noted in Fig. 2) for a single system may appear elusive. However, an examination of a variety of experimental systems allows one to assemble various 'snapshots' of each of the individual situations in[1] "...a metallic divided state."

Acknowledgements

I would like to thank my colleagues A C Curtiss, D G Duff, D A Jefferson, BFGJ Johnson, D E Logan and J M Thomas at Cambridge for their enthusiastic support and collaboration. I would also like to thank Professor J M Thomas for kindly supplying Part of Fig. 1. This work has been supported by S.E.R.C. and Johnson-Matthey Research Ltd. Finally I would like to thank both Professor C N R Rao as President of the Indian National Science Academy for the very kind invitation to visit India, and The Royal Society for Travel Funds.

References

1. M Faraday *Phil Trans* **147** (1857) 145
2. A C Curtis D G Duff P P Edwards D A Jefferson B F G Johnson and D E Logan *ms in preparation* (1985)
3. B F G J Johnson *Transition Metal Clusters* Wiley Chichester (1980)
4. G Schmid R Pfeil R Buese F Bandermann S Meyer G H M Calis and J W A van der Velden *Chem Ber* **144** (1981) 3634
5. J A A J Perenboom P Wyder and F Meier *Phys Rep* **78** (1981) 173
6. M R Harrison and P P Edwards In : *The Metallic and Nonmetallic States of Matter* Taylor and Francis London (1985) p 389
7. P P Edwards and C N R Rao (Ed) *The Metallic and Nonmetallic States of Matter* Taylor and Francis London (1985)
8. N F Mott *Phil Mag* **6** (1961) 287
9. T V Ramakrishan in ref. 7 (1985) p. 23
10. D M Wood and N W Ashcroft *Phys Rev B* **25** (1982) 6255
11. A F Ioffe and A R Regel *Progr Semicond* **4** (1960) 237
12. W A Curtin and N W Ashcroft *Phys Rev B* **31** (1985) 3287
13. R Kubo *J phys Soc Japan* **17** (1962) 975
14. R Kubo A Kawabata and S Kobayashi *Ann Rev Mater Sci* **14** (1984) 49
15. J A A J Perenboom *et al* ref. 5 p. 192
16. J M Ziman *Electrons and Phonons* Clarendon Press, Oxford (1960)
17. G T Meaden *Electrical Resistance of Metals* Heywood London (1966)
18. T Fujita K Ohshima and T Kuroishi *J phys Soc Japan* **40** (1976) 90
19. K Ohshima T Fujita and T Kuroishi *J Phys Paris (collogne)* **38** (1977) C2-163
20. R N Edmonds P P Edwards S C Guy and D C Johnson *J phys Chem* **88** (1984) 3764

21. R N Edmonds and P P Edwards *Proc R Soc* **A 395** (1984) 341
22. R J Elliott *Phys Rev* **96** (1954) 266
23. Y Yafet *Solid State Phys* **14** (1963) 1
24. D E Logan and P P Edwards *to be published*
25. S C Guy R N Edmonds and P P Edwards *J chem Soc Faraday Trans* (II) **81** (1985) 937
26. M Smithard *Solid State Commun* **14** (1974) 407; 411
27. P P Edwards M R Harrison J Klinowski S Ramdas J M Thomas D C Johnson and C J Page *J chem Soc Chem Commun* (1984) 982
28. M R Harrison P P Edwards J Klinowski and J M Thomas *J Solid State Chem* **54** (1984) 330
29. M R Harrison P P Edwards J Klinowski and J M Thomas *Proc R Soc* (1986) *to be submitted*
30. F J DiSalvo J V Waszczak M R Harrison J M Thomas and P P Edwards *unpublished observations* (1985)
31. R N Edmonds M R Harrison and P P Edwards *J Chem Soc Faraday Trans* in Press (1985)
32. D C Johnson R E Benfield P P Edwards W J Nelson and M D Vargas *Nature* **314** (1985) 231
33. B K Teo *Private communications* (1985)
34. A Ceriotti F Demartin G Longoni M Manassero M Marchionna G Piva and M Sansoni *Angew Chem int Edn Engl* **24** (1985) 697
35. N C Pyper and P P Edwards *J chem Soc Chem Commun* submitted (1985)
36. A C Curtis D G Duff P P Edwards D A Jefferson B F G Johnson and D E Logan *unpublished observations* (1985)
37. C N R Rao *Solid State Chemistry—A Perspective Report* Indian National Science Academy New Delhi (1984) p 1
38. M Beer R W Carpenter L Eyring C E Lyman and J M Thomas *Chem Eng News* **59** (1981) 40